Probability Distributions of Gas Hydrate Formation

Reuben Wu
CSIRO Materials Science and Engineering, Ian Wark Laboratory, Bayview Avenue, Clayton, VIC3168, Australia

Centre for Energy, School of Mechanical and Chemical Engineering, The University of Western Australia, M050 Crawley, WA6009, Australia

Karen A. Kozielski
CSIRO Earth Science and Resource Engineering, Ian Wark Laboratory, Bayview Avenue, Clayton, VIC3168, Australia

Patrick G. Hartley
CSIRO Materials Science and Engineering, Ian Wark Laboratory, Bayview Avenue, Clayton, VIC3168, Australia

Eric F. May and John Boxall
Centre for Energy, School of Mechanical and Chemical Engineering, The University of Western Australia, M050 Crawley, WA6009, Australia

Nobuo Maeda
CSIRO Materials Science and Engineering, Ian Wark Laboratory, Bayview Avenue, Clayton, VIC3168, Australia

DOI 10.1002/aic.14037
Published online February 25, 2013 in Wiley Online Library (wileyonlinelibrary.com)

Induction time distributions for gas hydrate formation were measured for gas mixtures of methane + propane at pressures up to 11.3 MPa using a high-pressure automated lag time apparatus (HP-ALTA). Measurements were made at subcooling temperatures between 4.3 and 13.5 K and, while isothermal induction times between 0 and 15,000 s were observed, the median isothermal induction times for the distributions ranged from 100 to 4000 s. A hyperbolic relationship between median induction time and subcooling was used to correlate the data. A graphical interpretation is presented that relates the two types of data that can be acquired by using the HP-ALTA in one of two modes to study hydrate formation: induction time distributions at constant subcooling and formation temperature distributions observed during linear cooling ramps. The equivalence of these two modes provides a robust method for studying the variation of formation phenomena in different hydrate systems. © 2013 American Institute of Chemical Engineers *AIChE J*, 59:2640–2646, 2013

Keywords: hydrate, nucleation, crystal growth, induction time, subcooling

Introduction

Gas hydrates are crystalline solids that form when gas molecules are enclosed in a hydrogen-bonded network of water molecules under conditions of low temperatures (273–300 K) and high pressures (above 0.6 MPa).[1] The formation of gas hydrates in pipelines can cause blockages and is a major problem in the oil and gas industry.[2] Therefore, an understanding of formation mechanisms is essential in the development of accurate hydrate prediction models and in the design of hydrate avoidance or remediation procedures.

Studies on the formation (nucleation and growth) of an emerging phase generally require statistical analyses of large sets of data because of the stochastic (nondeterministic) nature of the nucleation process.[3–5] For the case of the formation of gas hydrates, isothermal measurements at a constant subcooling are commonly carried out and the observed distribution of induction times provides a measure that characterizes their formation.[6,7] However, such experiments have been shown to be time consuming, apparatus dependent, and the results highly stochastic.

For ice nucleation, Haymet and coworkers introduced a new method of collecting such statistics. They described in a series of articles the design and operation of an ambient pressure automated lag-time apparatus (ALTA) which was capable of automatically collecting large amounts of data from a single sample in a relatively short period of time.[5,8,9] Using the ALTA, a single sample was cooled until freezing was detected, at which point a heating cycle was initiated to restore the sample back to its original state. This cooling/heating cycle can be repeated as many times as desired to generate the required statistics. The linear increase in subcooling used in the ALTA experiments enabled data to be collected more quickly than during isothermal induction time measurements because the sample is subjected to a continually increasing driving force. The statistical data on the

Correspondence concerning this article should be addressed to N. Maeda at Nobuo.Maeda@csiro.au.

formation of ice collected in this manner during an ALTA experiment are not in the form of a collection of isothermal induction times but rather in the form of a collection of (maximum) subcooling temperatures achieved.

For these two forms of statistical nucleation data to be comparable with each other, the establishment of a correlation between these two quantities is essential. Heneghan et al.[5] measured the distribution of isothermal induction times for the formation of AgI-seeded ice at three different subcooling temperatures. They showed average isothermal induction times as a function of (constant) subcooling. Three functional forms of the relation, exponential, power law, and classical nucleation theory, were shown to give an equally good fit of the data. In a subsequent article, they operated the ALTA using the linear cooling method and showed that the same isothermal induction time—subcooling curve could be extracted from a single "survival curve."[9] A "survival curve" is a collection of subcooling temperatures of hundreds of individual experimental runs and, when appropriately rearranged, constitutes a probability distribution of ice nucleation expressed in terms of subcooling temperatures. The median of the distribution is then usually cited as the most likely (representative) subcooling temperature for nucleation for a given sample. The ALTA was then applied to the study of a model THF hydrate.[10]

Maeda et al. recently reported the development of the high-pressure version of an automated lag time apparatus (HP-ALTA) for the study of gas hydrate nucleation and growth at elevated gas pressures. The survival curve probability distribution for gas hydrate formation was predominantly determined by that of nucleation (as opposed to that of growth).[11] This HP-ALTA was then used to study the formation (nucleation and growth) of interfacial hydrate films of three gases: methane, 10 mol% propane 90 mol% methane (C1/C3) mixed gas, and a synthetic gas mix consisting of methane, ethane, propane, and n-butane.[12] They obtained probability distributions of the hydrate formation temperatures (T_f) at different gas pressures and cooling rates, and found that T_f generally increased with gas pressure. They also showed that a minimum threshold pressure for hydrate formation exists for each gas studied.

One striking feature of the probability distribution of T_f of gas hydrates is that the range of distribution (typically 20 K) was much broader than that of ice (typically 3–4 K). The underlying physical reason for this is that unlike ice, for which the nucleation process is considered to be single-step, the nucleation of gas hydrates first requires build-up of sufficient gas supersaturation in the aqueous phase and hence is often mass transfer limited. This is due to the very low solubility of typically nonpolar gases in water. Consequently, the nucleation and the growth of gas hydrates in a quiescent sample take place at the water–gas interface, where the concentration of the gas in water is the highest. Since mass transfer of gas into the aqueous phase is required as an additional step in the nucleation and growth processes, this additional kinetic step causes the width of the probability distribution to be much larger in temperature than that in ice.[12] It is, therefore, not clear whether the correlation obtained by Heneghan et al.[5] for ice remains valid or applicable at all to gas hydrates because of this intrinsic difference in the mechanisms of nucleation and growth between ice (single-step process) and gas hydrates (two-step process).

In this work, we used an HP-ALTA to study the nucleation and growth of C1/C3 mixed gas hydrates in two different modes. In the first mode, we measured the subcooling temperatures of a system containing water and a C1/C3 gas mixture during linear cooling ramps. In the second mode, we measured the isothermal induction times prior to the formation of gas hydrates. We then derived an empirical correlation that connects these two quantities.

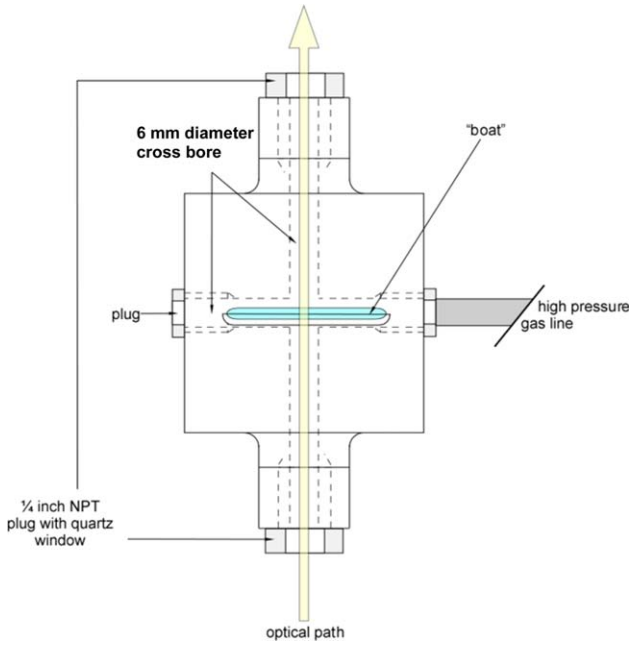

Figure 1. Schematic diagram showing the major components of the HP-ALTA in the "interfacial transmittance configuration."

[Color figure can be viewed in the online issue, which is available at wileyonlinelibrary.com.]

Materials and Methods

The C1/C3 mixed gas used in our experiments had the composition of (1 - z) CH_4 + z C_3H_8 with $z = 0.10 \pm 0.002$ by mole. The gas mixture was obtained from BOC Limited. Milli-Q water (18.2 MΩ resistivity) was used in all experiments.

The main components of the HP-ALTA are shown in Figure 1. For a detailed description of the modes of operation of the HP-ALTA, see Maeda et al.[11] Briefly, the water sample was placed in a glass sample cell ("boat") about 30 mm in length and 4 mm in width. The sample cell was placed in a stainless steel chamber and a light beam was passed through the sample vertically ("interfacial transmittance configuration"). The light passing through the sample was detected by a photodiode detector. Hydrate formation in a quiescent sample typically occurs at the gas–water interface in the form of a film due to the low solubility of gas in water. The formation of such a hydrate film caused the light beam to scatter, which would in turn result in a sudden decrease in the transmitted light intensity.

The HP-ALTA chamber was connected to a high pressure gas line via a Swagelok connection and pressurized using a pneumatically driven gas booster pump (Haskel Australasia Pty Ltd, Queensland, Australia, model number AG-62). The maximum pressure that could be studied was limited to 15 MPa by the pressure rating of the sodalime glass windows used in the instrument. The actual gas pressure was measured and monitored using a capacitance-diaphragm type pressure transducer (2200BGC1601A3UA, Gems Sensors, Basingstoke, England).

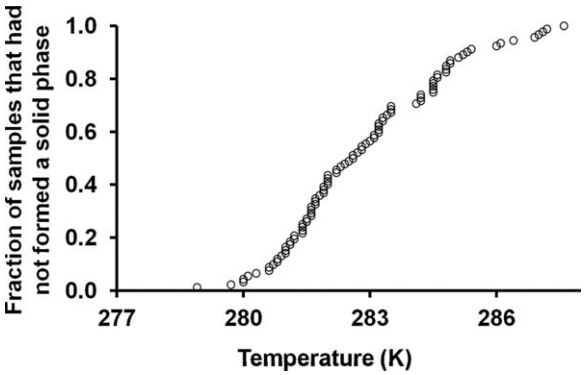

Figure 2. Typical survival curve for the C1/C3 mixed gas hydrate measured using a linear cooling ramp of 0.025 K/s at a gas holding pressure of 10.7 MPa, for which the hydrate equilibrium temperature is 296.1 K.

Heating and cooling of the sample was achieved using two Peltier modules (Peltier-CP1.4–127-06L-RTV, Melcor). A pair of heat sinks absorbed excess heat generated by the Peltier modules, which was then dissipated with the use of a refrigerated bath (Model WCR-P12, All-Lab Scientific). The actual temperature inside the HP-ALTA was measured and monitored using a platinum resistance thermometer (PT100 HEL705, Honeywell).

All experiments were conducted at isobaric conditions. When operating in the first of the two modes used, we allowed each cooling ramp to continue until hydrate formation was detected. After the detection of the hydrate formation, the instrument reheated the sample to a predetermined temperature, set at 10–15 K above the thermodynamic equilibrium dissociation temperature (T_{eq}) of the C1/C3 mixed gas hydrate at the experimental gas pressure (calculated using CSMGem[13]). The instrument then held the sample at that temperature for 300 s to ensure hydrate dissociation before the next cooling ramp commenced. This cooling/detection/heating cycle was repeated typically over 100 times for a given C1/C3 mixed gas pressure. We did not observe any systematic difference in our results between fresh, newly loaded samples and samples that had been cycled multiple times, which suggested that the heating conditions we used were sufficient to eliminate any "memory effect."[14]

Figure 2 shows a typical distribution of the hydrate formation temperature T_f ("survival curve") of C1/C3 mixed gas hydrate measured using a linear cooling ramp (cooling rate = 0.025 K/s) at a holding pressure, P_h, of 10.7 MPa. Heneghan and Haymet and Maeda et al. described the process of how the survival curves can be obtained using the data collected by an ambient pressure ALTA and by an HP-ALTA, respectively.[9,11] Hydrate formation was found to occur over a temperature range from 278 to 289 K at $P = 10.7$ MPa. The equilibrium hydrate dissociation temperature (T_{eq}) at $P_h = 10.7$ MPa is 296.1 K.[13]

The T_f distribution curves obtained from the first mode of operation were used to make initial estimates of the range of temperatures at which the "isothermal induction time" measurements should be carried out (the second mode of operation). The isothermal induction time is defined as the time elapsed from when the set holding temperature, T_h, is reached until hydrate formation is detected. This definition of isothermal induction time differs slightly from the definition of the "total induction time" (the total time experienced by a sample in the subcooled region) by the time required to reach T_h from T_{eq} during the cooling ramp. However, since a linear cooling ramp was used, these isothermal induction times can be readily converted to the total time experienced by a sample in the subcooled region. More importantly, the large cooling rate used, 0.025 K/s, meant the time spent cooling from T_{eq} to T_h was small (~200 to 500 s) compared with the timescale of the measured induction times (~1000 to 10,000 s). Hence, the difference caused by the slightly different definition of the induction time is unlikely to be significant. The extent of the significance can be quantitatively assessed from Figure 7.

The lower end of the survival curve corresponds to the lowest temperature at which an isothermal induction time measurement can be carried out, because hydrate formation was found to occur in all samples before reaching that temperature. The upper limit of temperature for an isothermal induction time measurement should be slightly above the top end of the survival curve. This is because hydrate formation can occur at a temperature slightly above the upper end of the survival curve if the sample were held at that temperature for sufficiently long time (as long as it is below T_{eq}). When the lower end of a survival curve extended below 273 K, we limited our measurements of the isothermal induction times to above 273 K so as to preclude the formation of ice.

The range of T_f observed for C1/C3 mixed gas hydrates typically extended over 20 K, which was much larger than that for ice or for THF hydrates (3–4 K).[10] This much larger range facilitated the present study by enabling a much wider range of T_h to be selected for the study of C1/C3 mixed gas hydrates.

The second mode of operation of HP-ALTA allowed automated detection and recording of isothermal induction times for C1/C3 mixed gas hydrate formation at various, constant subcooling temperatures. The pressure/temperature (P/T) conditions where we carried out these measurements are summarized in Figure 3. The solid curve is the thermodynamic equilibrium phase boundary of C1/C3 mixed gas hydrate dissociation which was calculated using CSMGem.[13] The location of the phase boundary relative to the measurement conditions establishes the driving force for nucleation and growth. As discussed by Kashchiev and Firoozabadi, the difference in chemical potential between the instantaneous and equilibrium states governs the driving force; this chemical potential difference is also referred to as the supersaturation.[15–17] The supersaturation is principally a function of actual concentration of dissolved gas in the aqueous solution; hence, the importance of mass transfer in determining when nucleation occurs. If the solution is assumed to be at an equilibrium concentration of dissolved gas, Kashchiev and Firoozabadi provide formulae for calculating the supersaturation from either the system subcooling (along an isobaric pathway) or from the system overpressure, $\Delta P \equiv P_h - P_{eq}$, (along an isothermal pathway). The supersaturation calculated via either method is the same; however, it is slightly more convenient and conventional to utilize the subcooling as a driving force proxy because ΔT is proportional to the supersaturation, in contrast with the overpressure, which varies logarithmically with supersaturation.[15]

Results

Figure 4a shows a histogram of isothermal induction times of C1/C3 mixed gas hydrate formation at $P_h = 4.3$ MPa and

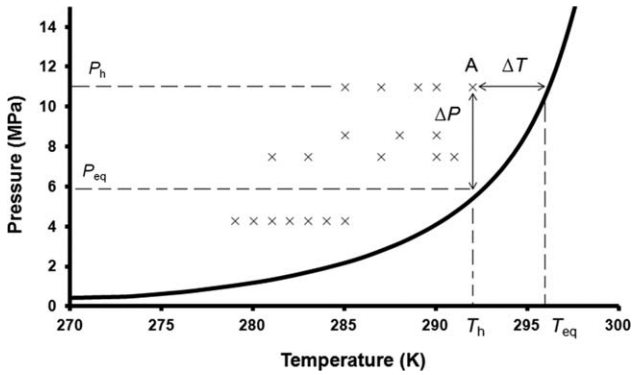

Figure 3. *P–T* diagram showing the equilibrium phase boundary for C1/C3 mixed gas hydrate, and the locations, ×, where the isothermal induction time measurements were conducted.

Point *A* is chosen to illustrate the relationships between subcooling, ΔT; equilibrium temperature, T_{eq}; the experimental holding temperature, T_h; the experimental holding pressure, P_h; and the system overpressure, ΔP. The driving force for nucleation at Point *A*, can be determined either from ΔT or from ΔP, assuming the gas concentration in the aqueous phase is at its equilibrium value.[15]

$T_h = 279$ K for 83 runs. The equilibrium dissociation temperature, T_{eq}, of C1/C3 mixed gas hydrate at 4.3 MPa was calculated to be 290 K. Isothermal induction times ranged from zero to 457 s. In cases where the C1/C3 mixed gas hydrate formed during the cooling ramp on the way to the target holding temperature of $T_h = 279$ K, the isothermal induction time was deemed to be zero. The maximum experimental time period was set at 15,000 s but hydrate formation was detected in all runs at this condition within this time.

Figure 4b shows a histogram of isothermal induction times for C1/C3 mixed gas hydrate formation at $P_h = 4.3$ MPa and $T_h = 284$ K for 114 runs. At this much smaller subcooling, the measured isothermal induction times had a much larger variation than at 279 K, ranging from 629 to 15,000 s. When no hydrate formation was detected within the maximum experimental time of 15,000 s, we deemed the isothermal induction time for that particular run to be 15,000 s. The bias introduced by this experimental constraint was partially offset by considering the median observed induction time as opposed, for example, to the mean induction time.

The distribution of isothermal induction times can also be presented in the form of "survival curves." Figure 4c shows a series of example survival curves measured at $P_h = 4.3$ MPa, 279 K $\leq T_h \leq$ 284 K. It shows the fraction of the number of samples which had formed C1/C3 mixed gas hydrate after a given isothermal induction time (subtly different from subcooling survival curves, such as Figure 2, where the ordinate is the fraction of samples that had not formed hydrate). For the experiments at $T_h = 284$ K, C1/C3 mixed gas hydrate often did not form in the first 15,000 s (see Figure 4b); consequently, the fraction of sample that had formed hydrate remained well below 1 even at the maximum 15,000 s isothermal induction time. Figure 4c indicates that as T_h decreased (subcooling increased), (1) isothermal induction times became shorter, (2) the size of the distribution of isothermal induction times decreased, (narrower curve) and (3) the fraction of runs in which hydrate formed at any given time increased.

Isothermal induction time measurements were carried out at several different pressures and holding temperatures. Figure 5 shows the relationship between the median isothermal induction times as a function of T_h for several values of P_h. The median isothermal induction time observed at a given T_h decreased as the P_h increased because of greater subcooling and, thus, driving force. The induction time distribution's median was chosen as the representative measure of a data set at each P/T condition because of the maximum

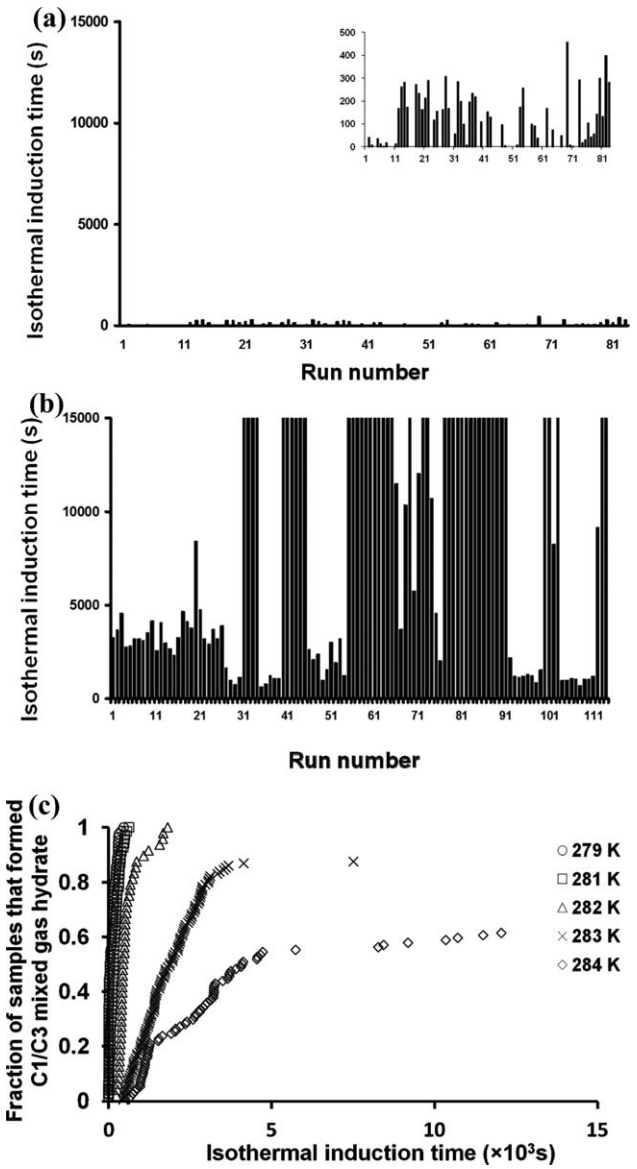

Figure 4. Isothermal induction times for C1/C3 mixed gas hydrate measurements.

(a) Histogram for 83 runs at $T_h = 279$ K and $P_h = 4.3$ MPa, for which $T_{eq} = 290$ K. The maximum isothermal induction times measured at this condition was 457 s. Induction times of zero were recorded for experiments in which formation occurred before T_h was reached. The inset shows the data replotted with a vertical scale from 0 to 500 s. (b) Histogram for 114 runs at $T_h = 284$ K and $P_h = 4.3$ MPa. The minimum isothermal induction time measured at this condition was 629 s. Induction times of 15,000 s were recorded for experiments which were terminated after the maximum experimental period. (c) Isothermal induction time survival curves for $P_h = 4.3$ MPa and 279 K $\leq T_h \leq$ 284 K.

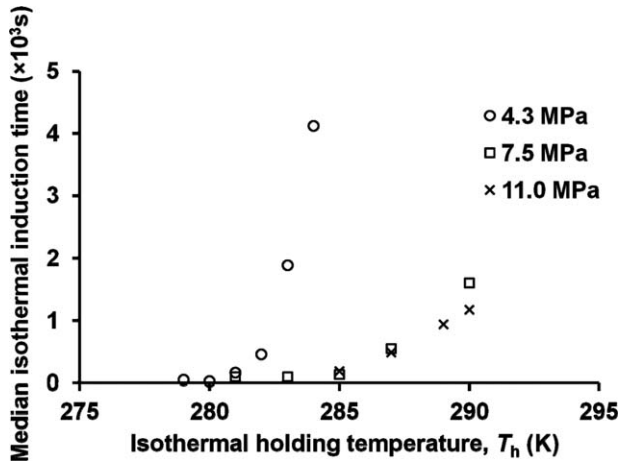

Figure 5. Median isothermal induction times as a function of T_h at a selection of different P_h.

The equilibrium hydrate temperatures were 290, 294, and 296 K for the holding pressures of 4.3, 7.5, and 11.0 MPa, respectively.

experimental observing time limitation. The use of the distribution's median also has an advantage in that it is not greatly affected by the specific values of the isothermal induction times recorded, as long as more than 50% of the samples formed C1/C3 mixed gas hydrates before 15,000 s, which was the case at all *P*/*T* conditions in this study.

Discussion

Figure 6a shows the median of *total* induction times plotted as a function of subcooling ΔT. The conversion from isothermal to total induction times has little effect given the relatively fast cooling ramps utilized in this work.* For $\Delta T < 9$ K, the data appear to separate into two branches, with the "lower" branch corresponding to an apparently "easier" formation process. Also shown in Figure 6a are the data of Heneghan et al. (×) who reported three average isothermal induction times for ice formation at atmospheric pressure measured using an ALTA.[5] Interestingly, the ice formation data are in reasonable agreement with the "upper" branch of median induction times for C1/C3 mixed gas hydrate formation.

The agreement between the data of Heneghan et al. and the "upper branch" of our data leads to the question of whether there is some generality to be drawn from this result.[5] The apparatus used in both cases had some similarities and the mass transfer limitation effect is suppressed in isothermal induction experiments with hydrates, which might explain the similarities with the ice experiment. The difference between the one-step and two-step nucleation mechanisms is most pronounced in cooling ramp experiments, as manifest in the large differences in survival curve distribution width observed for gas hydrates and ice (or THF hydrates).[5,10,12] This is because in such experiments the solubility of the gas in the water increases with decreasing temperature. Thus, increasing amounts of gas in the aqueous phase are required as the ramp proceeds to attain the given level of supersaturation necessary for nucleation. The faster the cooling rate, the more severe this shortfall in the gas concentration at a given subcooling, and the more that mass transfer can limit the nucleation. In contrast, however, during isothermal induction time measurements, the gas solubility does not change with time and thus mass transfer is not as great a limitation as during a cooling ramp. Therefore, the nucleation mechanism could effectively become one-step (similar to ice formation), especially for longer induction

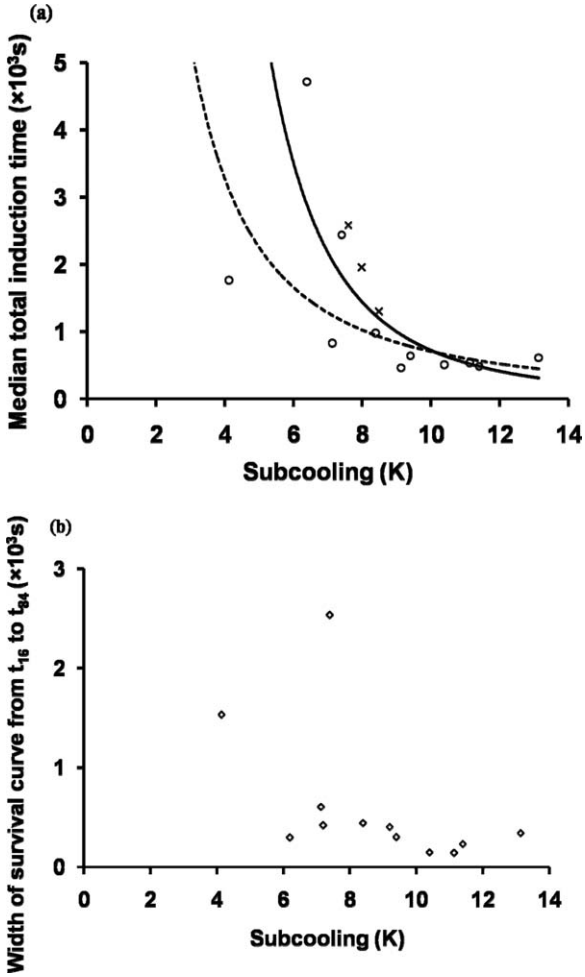

Figure 6. Median and widths of total induction time survival curves for C1/C3 mixed gas hydrates plotted as a function of the subcooling of the system, ΔT.

(a) Median induction times which generally shortened as the subcooling was increased. The three data points (×) obtained by Heneghan et al.[5] for the average isothermal induction time of ice formation at atmospheric pressure are also shown. The curves represent power law functions corresponding to Eq. 1 fitted to the data, with best-fit parameters listed in Table 1. The dashed curve corresponds to the function fit to all data measured in this work, whereas the solid curve is fit only to the upper branch data. (b) Width of the survival curves measured from t_{16} to t_{84} plotted as a function of subcooling, where t_{16} is the time by which 16% of the total number of samples formed hydrate and t_{84} is the time by which 84% of the total number of samples formed hydrate. If we consider the two points at subcoolings 4 K and 7 K as outliers, the widths of the other survival curves from range from 140 to 605 s, with an average of 330 s.

*The difference between the use of the "isothermal induction time" and the "total induction time" can be quantitatively expressed by the gap between a colored straight line that simulates a linear cooling ramp and the x-axis, as shown in Figure 7 (the conversion of "isothermal induction time" to "total induction time" shifts the data points vertically upward by the size of the gap).

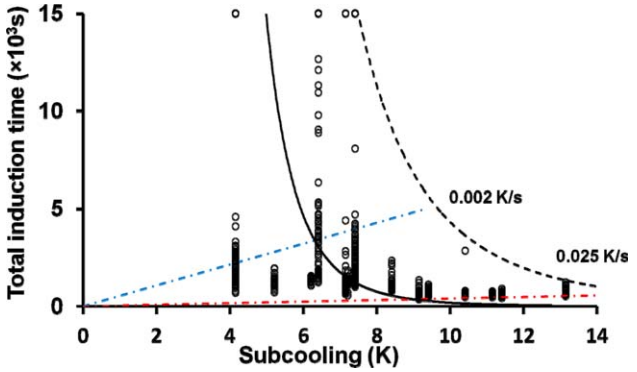

Figure 7. Total induction times for each individual run as a function of subcooling, ΔT.

The solid curve corresponds to Eq. 1 with the second set of (A,p) parameters listed in Table 1 (this curve is the same as the solid curve in Figure 6a). Here, the dashed curve corresponds to a rough estimate of a spinodal beyond which hydrate nucleation becomes labile. The two colored straight lines from the origin simulate linear cooling ramps which correspond to the cooling rates of 0.025 K/s (red; actual experimental cooling rate used in this study) and 0.002 K/s (blue). A "survival curve" (Figure 2) constructed from hundreds of automated linear cooling ramps in an HP-ALTA is essentially a distribution of data points on such a straight line. [Color figure can be viewed in the online issue, which is available at wileyonlinelibrary.com.]

times. This could explain the agreement between some of our isothermal induction time data and those of Heneghan et al.[5]

Nevertheless, even with a suppression of the mass-transfer component of the two-step formation mechanism, the data of Heneghan et al. would be expected to fall on the left side of our data as the one-step required for ice formation should remain faster.[5] Furthermore, the apparent ease of formation observed for two of the data sets measured in this work at $\Delta T < 7.5$ K ("lower" branch in Figure 6a) indicates that apparatus effects, or other experimental systematics that occurred despite the precautions taken, may have played a dominant role in those experiments. Such systematics may include taking an insufficient number of data at that condition, or the influence of the memory effect.[14] Hence, the agreement between our data and those of Heneghan et al. should probably be considered fortuitous until further evidence to the contrary is obtained.

Following Heneghan et al., a power law (hyperbolic) was chosen to represent the relationship between the median total induction time, t_{med}, and the subcooling:

$$t_{\mathrm{med}} = \frac{A}{(\Delta T - 3\mathrm{K})^p} \tag{1}$$

Here, A and p are empirical constants that were treated as adjustable parameters determined by least squares regression to measured data. Either a power law or an exponential function can fit our data equally well. However, Maeda et al. observed a minimum subcooling threshold of about 3 K for each of the three gas hydrates they studied with this apparatus.[12] For this reason, we chose a hyperbolic power law function that is asymptotic to the induction time axis with an offset of 3 K. Also, while Heneghan et al. correlated *mean* total induction times as a function of subcooling, for the reasons discussed above we correlated *median* total induction times with subcooling.[5] Table 1 lists two sets of (A, p) values determined by regression to two (t_{med}, ΔT) data sets.

The results of these two of the fits are shown in Figure 6a: neither fit included the data of Heneghan et al.[5] The first set of (A, p) values in Table 1 were derived from a fit to all the data in Figure 6a (dashed curve). Such a fit assumes that all of the median total induction time data should be weighted equally. The second set of (A,p) values were derived by repeating the fit but excluding the two hydrate data sets for $\Delta T < 7.5$ K which lie on the "lower" branch. This exclusion is based on the premise that hydrate formation in these data sets occurred anomalously quickly relative to the majority of the data as a result of hitherto unknown factors such as the memory effect.

Figure 6b shows the width of the measured isothermal survival curves as a function of subcooling. The widths of the survival curves are given by the difference between t_{16} and t_{84}, which are the times at which 16% and 84% of the number of total samples had formed hydrate, respectively. The width contains the middle 68% of the data and is thus similar to showing the standard deviation of the distributions centered about the median. The data for which more than 16% of the runs resulted in reaching the cutoff 15,000 s without hydrate formation were not included in the analysis. The width of most of the survival curves range from 140 to 640 s, with the average calculated to be 330 s (if the two points at about 4 and 7 K subcooling are considered as outliers).

The specific values of the empirical parameters A and p, as well as the 3 K minimum subcooling asymptote in Eq. 1, are presumably specific to the apparatus and method followed in this work to some degree; while the similar results of Heneghan et al.[5] for ice nucleation may suggest similarities exist for measurements conducted using the ALTA method, the subcooling–induction time relationships observed in other hydrate formation experiments (e.g., high-pressure differential scanning calorimetry) differ significantly.[18] However, such a relationship is of value even if it is limited to a particular apparatus because it enables an equivalency to be established between scanning measurements of subcooling and induction time measurements at constant subcooling. Depending on the apparatus, the former method may be more efficient and produce more reliable results when quantitatively assessing the performance of kinetic hydrate inhibitors, than the more conventional latter method. Once the relationship is known, the same apparatus could also be used to investigate more efficiently differences in the formation properties of different hydrate systems, such as the effects of hydrate structure and gas composition.

To elucidate further the relationship between subcooling and induction time, as well as illustrate an operational boundary for this apparatus, Figure 7 shows the set of total induction times measured for each subcooling (i.e., not the median of the distribution of induction times). The dashed curve in Figure 7 represents a quasi boundary, which

Table 1. Sets of A and p Values for Eq. 1. Set 1 gives the Fit through all the Data Measured in this Work, Whereas Set 2 gives the Fit for the "Upper"' Branch in Figure 6.

	A	p
All data	3×10^5	2.40
Upper branch	2×10^5	4.01

provides a rough estimate of a spinodal beyond which hydrate nucleation becomes labile. For comparison, the solid curve in Figure 6, corresponding to the relationship between the median induction time and the subcooling for the second set of (A,p) values, is also shown in Figure 7.

The two colored straight lines from the origin in Figure 7 have been chosen to illustrate linear cooling ramps with rates of 0.025 K/s (red; actual experimental cooling rate used in this study) and 0.002 K/s (blue). As a sample is linearly cooled, hydrate formation may occur at any point along such a straight line. If the process were to be repeated for hundreds of times, the resulting distribution of T_f on the straight line would constitute a "survival curve" measured by an HP-ALTA, such as in Figure 2. We note that currently the HP-ALTA cannot operate at a cooling rate below 0.005 K/s or above 0.075 K/s.

The intersection between a straight line and the solid curve provides an estimate of the median of the survival curve measured for a cooling ramp. It can be seen from Figure 7 that, as the cooling rate increases, the median of a survival curve progressively shifts to a larger ΔT. For example, a cooling rate of 0.002 K/s would give a median subcooling of $\approx$6 K and a cooling rate of 0.025 K/s would give a median subcooling of $\approx$9 K. The latter graphically deduced value of the median subcooling is consistent with the median subcoolings of 8–14 K reported by Maeda et al. for C1/C3 mixed gas hydrates measured using the cooling ramp mode at rates from 0.025 to 0.05 K/s.[12]

Likewise, the maximum subcooling likely to be achieved during a linear cooling ramp could be estimated by the intersection of the straight line and the dashed curve in Figure 7. The faster the cooling rate, the greater the length of the straight line prior to its intersection with the dashed curve. The survival curve determined from such a cooling ramp would be broader and extend to larger subcoolings. For example, a cooling rate of 0.002 K/s would give a maximum subcooling of $\approx$9 K compared to a maximum subcooling of $\approx$15 K with the use of 0.025 K/s cooling rate. However, other constraints can limit the maximum subcooling achievable in practice such as the requirement to terminate experiments at 273 K to preclude ice formation.

Conclusion

While generally the relationship between isothermal induction time and subcooling is apparatus and method specific, such a relationship is of value because it establishes an equivalency between the linear subcooling measurements and the isothermal measurements. The driving force for gas hydrate formation depends on sufficient gas supersaturation in the aqueous phase which makes the nucleation mechanism for gas hydrates a two-step process as opposed to the one-step process for ice and THF hydrate formation. The mass transfer of gas to the gas–water interface then becomes the limiting step in the nucleation process. This is more pronounced when the linear subcooling method is used, since gas solubility increases with decreasing temperature and higher amounts of gases are then required to attain the necessary level of supersaturation. This explains why the survival curves of gas hydrate formation are wider than that of ice and THF hydrate formation. During the isothermal induction time measurements, in contrast, gas solubility remains constant and hence the build-up of gas supersaturation would be easier than during the cooling ramps. We believe that the agreement between some of our isothermal induction time data and the data of Heneghan et al. for ice formation was aided by this factor. In this work, we used a hyperbolic function to represent the relationship between the median induction time and subcooling of C1/C3 mixed gas hydrate formation.

Acknowledgments

This work was supported by NM's Australian Research Council Future Fellowship (FT0991892) and CSIRO's Petroleum and Geothermal Research Portfolio.

Literature Cited

1. Sloan ED. Fundamental principles and applications of natural gas hydrates. *Nature*. 2003;426:353–359.
2. Hammerschmidt EG. Formation of gas hydrates in natural gas transmission lines. *Ind Eng Chem*. 1934;26:851–855.
3. Parody-Morreale A, Bishop G, Fall R, Gill SJ. A differential scanning calorimeter for ice nucleation distribution studies—application to bacterial nucleators. *Anal Biochem*. 1986;154:682–690.
4. Vali G. Freezing rate due to heterogenous nucleation. *J Atmos Sci*. 1994;51:1843–1856.
5. Heneghan AF, Wilson PW, Wang GM, Haymet ADJ. Liquid-to-crystal nucleation: automated lag-time apparatus to study supercooled liquids. *J Chem Phys*. 2001;115:7599–7608.
6. Skovborg P, Ng HJ, Rasmussen P, Mohn U. Measurement of induction times for the formation of methane and ethane gas hydrates. *Chem Eng Sci*. 1993;48:445–453.
7. Natarajan V, Bishnoi PR, Kalogerakis N. Induction phenomena in gas hydrate nucleation. *Chem Eng Sci*. 1994;49:2075–2087.
8. Barlow TW, Haymet ADJ. Alta—an automated lag-time apparatus for studying the nucleation of supercooled liquids. *Rev Sci Instrum*. 1995;66:2996–3007.
9. Heneghan AF, Haymet ADJ. Liquid-to-crystal nucleation: a new generation lag-time apparatus. *J Chem Phys*. 2002;117:5319–5327.
10. Wilson PW, Lester D, Haymet ADJ. Heterogeneous nucleation of clathrates from supercooled tetrahydrofuran (THF)/water mixtures, and the effect of an added catalyst. *Chem Eng Sci*. 2005;60:2937–2941.
11. Maeda N, Wells D, Becker NC, Hartley PG, Wilson PW, Haymet ADJ, Kozielski KA. Development of a high pressure automated lag time apparatus for experimental studies and statistical analyses of nucleation and growth of gas hydrates. *Rev Sci Instrum*. 2011;82:065109.
12. Maeda N, Wells D, Hartley PG, Kozielski KA. Statistical analysis of supercooling in fuel gas hydrate systems. *Energy Fuels*. 2012;26:1820–1827.
13. Ballard L, Sloan ED. The next generation of hydrate prediction IV—a comparison of available hydrate prediction programs. *Fluid Phase Equilib*. 2004;216:257–270.
14. Buchanan P, Soper AK, Thompson H, Westacott RE, Creek JL, Hobson G, Koh CA. Search for memory effects in methane hydrate: structure of water before hydrate formation and after hydrate decomposition. *J Chem Phys*. 2005;123:164507.
15. Kashchiev D, Firoozabadi A. Nucleation of gas hydrates. *J Cryst Growth*. 2002;243:476–489.
16. Kashchiev D, Firoozabadi A. Driving force for crystallization of gas hydrates. *J Cryst Growth*. 2002;241:220–230.
17. Kashchiev D, Firoozabadi A. Induction time in crystallization of gas hydrates. *J Cryst Growth*. 2003;250:499–515.
18. Davies SR, Hester KC, Lachance JW, Koh CA, Sloan ED. Studies of hydrate nucleation with high pressure differential scanning calorimetry. *Chem Eng Sci*. 2009;64:370–375.

Manuscript received Sept. 17, 2012, and revision received Jan. 6, 2013